Reducing Surface Wetness Leads to Tropical Hydrological Cycle Regime Transition

Bowen Fan[1], Zhihong Tan[2], Tiffany A. Shaw[1], Edwin S. Kite[1]

[1]Department of the Geophysical Sciences, University of Chicago, Chicago, Illinois
[2]Program in Atmospheric and Oceanic Sciences, Princeton University, Princeton, New Jersey

Key Points:

- The tropical hydrological cycle exhibits a wet-to-dry regime transition when surface wetness is reduced in a general circulation model.
- Re-evaporation of stratiform precipitation causes the regime transition by impacting near-surface relative humidity.
- Re-evaporation happens at cloud base and the moistening effect diffuses to the near surface.

Corresponding author: Bowen Fan, bowen27@uchicago.edu

Abstract

The modern "wet" tropics are dominated by the Intertropical Convergence Zone, however "dry" tropics likely occurred in Earth's history. It is unclear how the tropics change between wet and dry climates because recent progress has focused on modern and warmer climates. We show the tropical hydrological cycle undergoes a wet-to-dry regime transition when surface wetness is decreased in a general circulation model. The dry regime occurs when precipitation is suppressed by negative evaporation. The regime transition is dominated by near-surface relative humidity, in contrast to our traditional understanding which assumes changes in relative humidity are small. We show near-surface relative humidity changes are controlled by re-evaporation of stratiform precipitation. The moistening effect of re-evaporation is non-local: re-evaporation happens near the lifting condensation level and moisture diffuses downward to the near-surface. Our results provide a first step toward understanding tropical hydrological cycle changes between wet and dry climates.

Plain Language Summary

Earth's modern tropical region is warm and wet, however it was likely dry in the past icy period. Here we investigate how the tropical hydrological cycle changes in response to reducing surface wetness in a state-of-the-art climate model with an idealized surface boundary. In response to reduced surface wetness, the tropics transitions from a wet regime (precipitation and evaporation are positive) to a dry regime (precipitation is negligible and evaporation is negative). Surprisingly, this regime transition is controlled by the re-evaporation of rain near cloud base. In the dry regime, tropical rainfall is re-evaporated aloft and the water vapor is transported to the near-surface via diffusion and affects the relative humidity. The evaporation becomes negative because the near-surface air has more moisture than the dry surface. Our results represent the first step toward understanding tropical regime transitions between wet and dry climates.

1 Introduction

A defining feature of Earth's modern climate is that precipitation maximizes near the equator in the InterTropical Convergence Zone (ITCZ, Hartmann, 2016). In the wet modern tropics, precipitation exceeds evaporation and there is moisture flux convergence by the large-scale circulation. However, the hydrological cycle was different in past climates (Pierrehumbert, 2002; Schneider et al., 2014). For example, in simulations of dry Snowball Earth, evaporation exceeds precipitation in the tropics (Pierrehumbert, 2005; Abbot et al., 2013). Thus, both wet (modern Earth) and dry (Snowball Earth) tropics are possible on Earth. Understanding the wet/dry contrast is important for Earth and also for the habitability of other planets (e.g. Kodama et al., 2018, 2019).

Recently, significant progress has been made in understanding changes in the position, width and strength of the ITCZ (Schneider et al., 2014; Byrne et al., 2018), but the focus has mostly been on the modern and warmer wet climates. It is not clear how the tropical hydrological cycle changes as the climate dries out. Going beyond the modern climate regime is key to pushing the boundary of our understanding of the atmospheric circulation (Held, 2018).

Cronin and Chavas (2019) showed that the transition from a wet to dry surface can be parameterized using a surface wetness parameter. Surface wetness (β) appears in the equation for evaporation (E):

$$E = \rho C_K L_v V_s q_s^* (\beta - H) \tag{1}$$

where ρ is the density of near-surface air, C_K is the exchange coefficient of moisture, L_v is the latent heat of vaporization of water, V_s is surface wind speed, q_s^* is the saturation

specific humidity at the surface, and H is the near-surface relative humidity. Physically β is the mole fraction of water in the solution and a small β value corresponds to a surface with limited water and high salinity. In arid environments like Antarctic ponds β can be as small as 0.28 (Toner et al., 2017).

How does the tropical hydrological cycle change between wet and dry climates? If we follow hydrological cycle changes between modern and warmer climates and assume relative humidity changes are small (Schneider et al., 2010), one would predict tropical evaporation becomes negative when $\beta < H \approx 0.8$ assuming changes in all other terms in (1), which are sign definite, are small. In addition, if we assume the change in moisture flux convergence is small, then precipitation may be suppressed by the cancellation of negative evaporation and moisture flux convergence. However, the assumption of small relative humidity changes has been tested for warmer climates, not for drier climates.

As a first step toward determining how the tropical hydrological cycle changes between wet and dry climates, we investigate the response to decreased surface wetness in an aquaplanet general circulation model (GCM). We use the wetness parameterization of Cronin and Chavas (2019). In the following sections, we begin by introducing the GCM simulations and moisture budget analysis (Section 2). We then present and discuss the tropical precipitation response to decreasing β and compare it to the predicted response following the assumption of small changes in relative humidity (Section 3). We conclude the paper by summarizing our results and discussing directions for future work (Section 4).

2 Methods

2.1 GCM simulations

We use the finite volume dynamical core of the GFDL-AM2 GCM with an aquaplanet configuration (Anderson et al., 2004). The simulations are configured as follows: obliquity and eccentricity are set to zero, with no diurnal cycle; the mixed layer depth is 50 m with no ocean heat transport and no sea ice; greenhouse gas concentrations are CO_2 = 348 ppmv, CH_4 = 1650 ppmv, N_2O = 306 ppbv, CFC-11 = 0, and CFC-12 = 0; ozone distribution is set as in Blackburn and Hoskins (2013). All simulations are run for 60 years with 10 years of spin up.

Precipitation is produced by two schemes: 1) the relaxed Arakawa-Schubert scheme (Moorthi & Suarez, 1992), which represents deep convection, and 2) the Tiedtke-Roststayn-Klein prognostic cloud scheme (Tiedtke, 1993; Rotstayn, 1997; Jakob & Klein, 1999), which represents stratiform clouds. In the stratiform scheme, the re-evaporation of rain is calculated at each atmospheric layer by integrating the diameter-dependent evaporation rate of a single raindrop over the Marshall-Palmer droplet size distribution (Marshall & Palmer, 1948). Re-evaporation of rain only happens if relative humidity in the unsaturated part of the grid box RH_{clr} is less than a critical value RH_{evap}.

In order to understand the importance of re-evaporation of rain for the tropical hydrological cycle we set up mechanism denial experiments. Mechanism denial experiments involve disabling a physical effect in the model in order to test its importance. We disable the re-evaporation of rain in the stratiform scheme by setting RH_{evap} to 0. We can also disable the re-evaporation in the relaxed Arakawa-Schubert scheme, but that does not cause a significant change in the precipitation. Hereafter "w/ re-evap" refers to simulations with re-evaporation enabled, and "w/o re-evap" refers to simulations with re-evaporation disabled.

2.2 Moisture Budget

The hydrological cycle on Earth is controlled by the time-averaged moisture budget of the atmosphere:

$$P = -\nabla \cdot \vec{F_q} + E \tag{2}$$

where P is precipitation, and $-\nabla \cdot \vec{F_q}$ is column-integrated moisture flux convergence. We follow Cronin and Chavas (2019) and modify the bulk aerodynamic formula for surface evaporation [see equation (1)]. We carried out simulations with β = 0, 0.001, 0.003, 0.01, 0.03, 0.1, 0.3, 0.5, 0.7, and 1.0.

We focus on the response of tropical hydrological cycle defined by a meridional average over 5°S to 5°N, which encapsulates the width of the ITCZ (Supplementary Table 1). We use the δ notation to represent the difference between drier and wetter climates with different β values. e.g.

$$\delta E = E_{\beta_2} - E_{\beta_1} \tag{3}$$

where $\beta_2 < \beta_1$. The moisture budget response can be written as:

$$\delta P = -\nabla \cdot \delta \vec{F_q} + \delta E \tag{4}$$

where δP is the change of precipitation, $-\nabla \cdot \delta \vec{F_q}$ is the change of column-integrated meridional moisture flux convergence, and δE is the change of surface evaporation. Following equation (1), we can further decompose the evaporation response as:

$$\delta E \approx \rho C_K L_v V_s [q_s^* \delta\beta - q_s^* \delta H + (\beta - H)\delta q_s^* + \delta(\beta - H)\delta q_s^* + \cdots] \tag{5}$$

where terms on the right hand side represent the direct effect of decreasing surface wetness ($q_s^* \delta\beta$), the effect of near-surface relative humidity changes ($-q_s^* \delta H$), the effect of changes in saturation specific humidity [$(\beta - H)\delta q_s^*$] and finally the nonlinear effect of changes in saturation specific humidity and deviations of β from H [$\delta(\beta - H)\delta q_s^*$]. Other nonlinear terms are negligible (Supplementary Fig. 2).

3 Results

3.1 Regime transition of the tropical hydrological cycle

As surface wetness (β) decreases, the tropical hydrological cycle transitions from a wet to a dry regime (Fig. 1a). The wet regime occurs when the hydrological cycle corresponds to that of modern Earth, namely in the tropics evaporation (gray line, Fig. 1a) and moisture flux convergence (black dashed line, Fig. 1a) both contribute to precipitation (black line, Fig. 1a). The wet regime occurs when $\beta > 0.1$. The dry regime is identified when precipitation is small because negative evaporation (near-surface has more moisture than the surface) opposes moisture flux convergence. The dry regime occurs when $\beta \leq 0.1$ instead of $\beta < H \approx 0.8$ as expected assuming relative humidity changes are small (see Introduction).

The transition from wet to dry tropics is clearly controlled by the change of sign of evaporation. In order to understand the evaporation response, we decompose it into different contributions following equation (5). If the assumption of small relative humidity changes $\delta H \approx 0$ is correct, then $q_s^* \delta(\beta - H)$ (purple solid line, Fig. 1b) should be equal to $q_s^* \delta\beta$ (red dashed line, Fig. 1b). We find $q_s^* \delta(\beta - H)$ deviates from $q_s^* \delta\beta$ in the dry regime (compare purple line and red dashed line, Fig. 1b), and the wet to dry tropics regime transition follows $q_s^* \delta(\beta - H)$ (compare grey and purple lines, Fig. 1b), suggesting changes in relative humidity are important. The specific humidity changes (green solid line, Fig. 1b) and nonlinear changes (orange solid line, Fig. 1b) are large, but they cancel out.

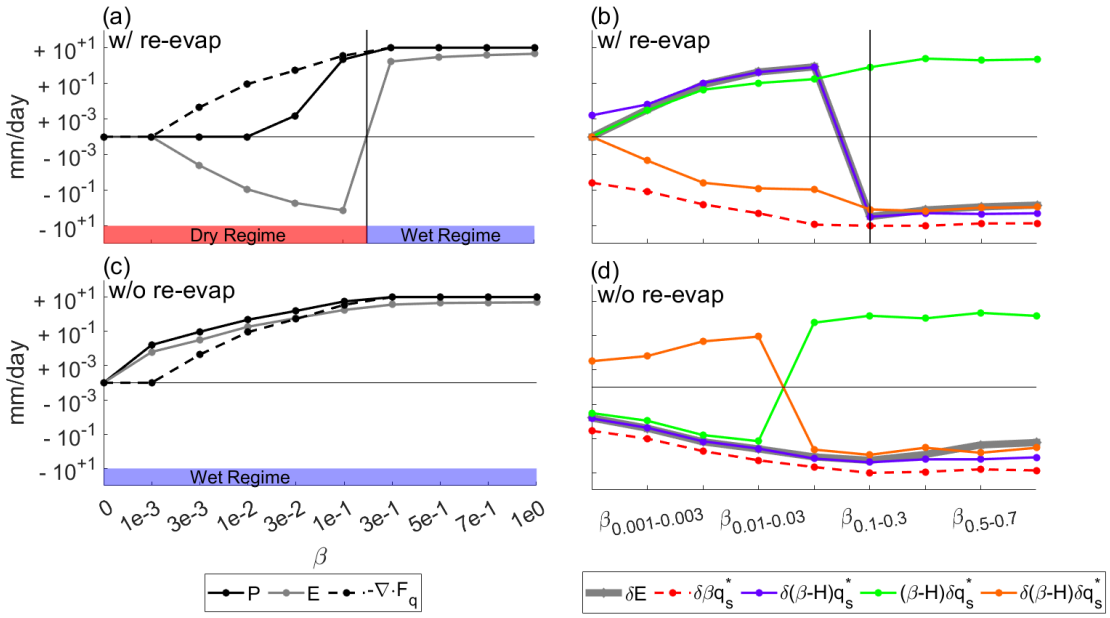

Figure 1. Time mean, zonal mean, and tropical mean (a) moisture budget and (b) decomposition of evaporation for simulations with re-evaporation enabled; (c,d) are similar to (a,b) but for simulations with re-evaporation disabled.

Overall, relative humidity changes are not small and follow changes in β (Fig. 2). The transition from wet to dry tropics can be identified using the relationship between β and H. For example, the wet regime occurs when $\beta > H$, while the dry regime occurs when $\beta < H$ (see blue line crossing black line, Fig. 2). Thus, the change of near surface relative humidity is fundamental to the wet to dry regime transition.

3.2 Role of re-evaporation for the wet-to-dry regime transition

Near-surface relative humidity clearly controls the wet-to-dry regime transition of the tropical hydrological cycle. Relative humidity is affected by many different factors including re-evaporation. Re-evaporation has been shown to have a large impact on the position of the ITCZ because re-evaporative cooling weakens the coupling between condensational heating and vertical motion (Bacmeister et al., 2006). Here we hypothesize re-evaporation controls the strength of the ITCZ and thus the wet-to-dry regime transition of the tropical hydrological cycle as surface wetness decreases.

We test the hypothesis using mechanism denial experiments (see section 2.1). When re-evaporation is disabled in the GCM simulations there is no regime transition and the wet regime occurs for all β values, i.e. evaporation is always positive (Fig. 1c). In the simulations with re-evaporation disabled, relative humidity changes are too small compared changes in β to account for the changes in evaporation, i.e. $q_s^*\delta(\beta - H)$ scales with $q_s^*\delta\beta$ (compare grey and red dashed lines, Fig. 1d) consistent with the assumption that relative humidity changes are small. Thus, without the moistening effect of re-evaporation, $\beta > H$ as β decreases (red line, Fig. 2).

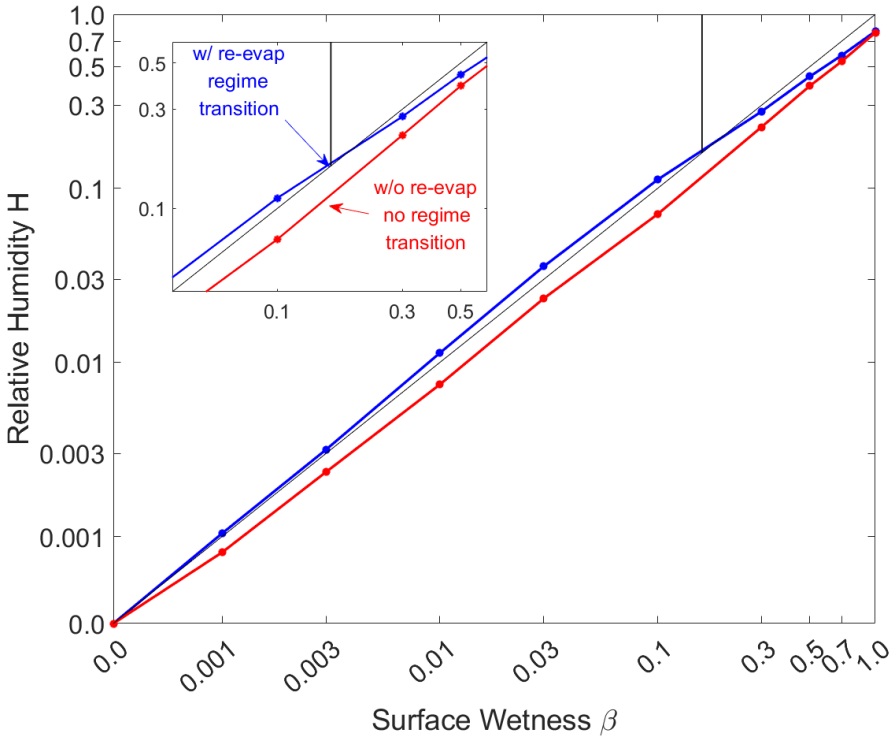

Figure 2. Near-surface atmospheric relative humidity H as a function of surface wetness β for simulations with and without re-evaporation. The thin black line from the bottom-left to the top-right is the one-to-one line. The wet regime occurs when $\beta > H$, while the dry regime occurs when $\beta < H$ as indicated by the vertical black line.

3.2.1 Impact of re-evaporation from stratiform precipitation

Is re-evaporation associated with stratiform or deep convective precipitation? In the GCM simulations, both deep convective and stratiform precipitation are suppressed as β decreases with re-evaporation enabled (Supplementary Fig. 1a). When $\beta < H$ precipitation (Supplementary Fig. 1a) and the moistening tendency due to re-evaporation in the deep convection scheme (compare Fig. 3a to Supplementary Fig. 3a) are negligible compared to those in the stratiform scheme. Disabling re-evaporation leads to enhanced stratiform precipitation but no impact on deep convective precipitation (Supplementary Fig. 1b). Consistently, the moistening tendency due to re-evaporation from stratiform precipitation dominates over that from the deep convection scheme (compare Fig. 3b to Supplementary Fig. 3b).

Does re-evaporation from stratiform precipitation moisten the near-surface air via local or non-local processes? The stratiform precipitation scheme output from the GCM suggests that re-evaporation moistens the air aloft (non-locally) as β decreases (see $dq/dt > 0$ in Fig. 3a). Moreover, when re-evaporation is disabled the moistening aloft does not occur (Fig. 3b). Note the positive moisture tendency without re-evaporation in the lower atmosphere is associated with turbulent mixing of cloud droplets and the unsaturated environmental air, leading to cloud erosion and moistening of the environment (Supplementary Fig. 4).

Why does re-evaporation occur aloft as β decreases? The level where re-evaporation from stratiform precipitation moistens the atmosphere (blue circles, Fig. 3c) follows the Lifting Condensation Level (LCL, red circles, Fig. 3c). The LCL is calculated using surface relative humidity and temperature following Romps (2017). The LCL calculation does not depend significantly on surface temperature which changes with β (compare red circles and stars, Fig. 3d). Thus, as surface relative humidity decreases following β, the near-surface air is further away from saturation and the LCL moves upward.

3.2.2 Role of vertical diffusion

How does moistening due to re-evaporation near the LCL reach the near surface and affect relative humidity? We hypothesize that vertical diffusion is important for getting the non-local moistening near the LCL to impact the near surface relative humidity. We test the hypothesis by looking at the moistening tendency due to vertical diffusion. Vertical diffusion clearly moistens the atmosphere below the LCL in the dry regime (Fig. 4).

In the GCM simulations, the specific humidity q is constant below the LCL (Supplementary Fig. 5) consistent with the Cloud Resolving Model (CRM) simulations of Cronin and Chavas (2019). If we assume the moistening tendency due to re-evaporation is balanced by vertical diffusion below the LCL then we obtain a vertical length scale $\mathcal{H}$:

$$\mathcal{H} = \sqrt{\kappa\tau} \tag{6}$$

where κ is diffusivity and τ is the time scale. We estimate the time scale using specific humidity just below the LCL and the maximum moistening tendency due to re-evaporation of stratiform precipitation:

$$\tau = \frac{q}{(dq/dt)_{max}}. \tag{7}$$

When using the diffusivity coefficient, maximum moistening tendency due to re-evaporation of stratiform precipitation (see Fig. 3a), and specific humidity below the LCL (Supplementary Fig. 5), the vertical length scale $\mathcal{H}$ is estimated to be 10-20 km (Table 1), which is on the order of the depth of the tropical troposphere. Our scaling of $\mathcal{H}$ can be treated as an upper limit. The actual vertical length scale $\mathcal{H}_{act}$ is defined as the height where $dq/dt_{vert-diff} = 0$ (see Fig. 4). Since the estimated vertical length scale is of the same

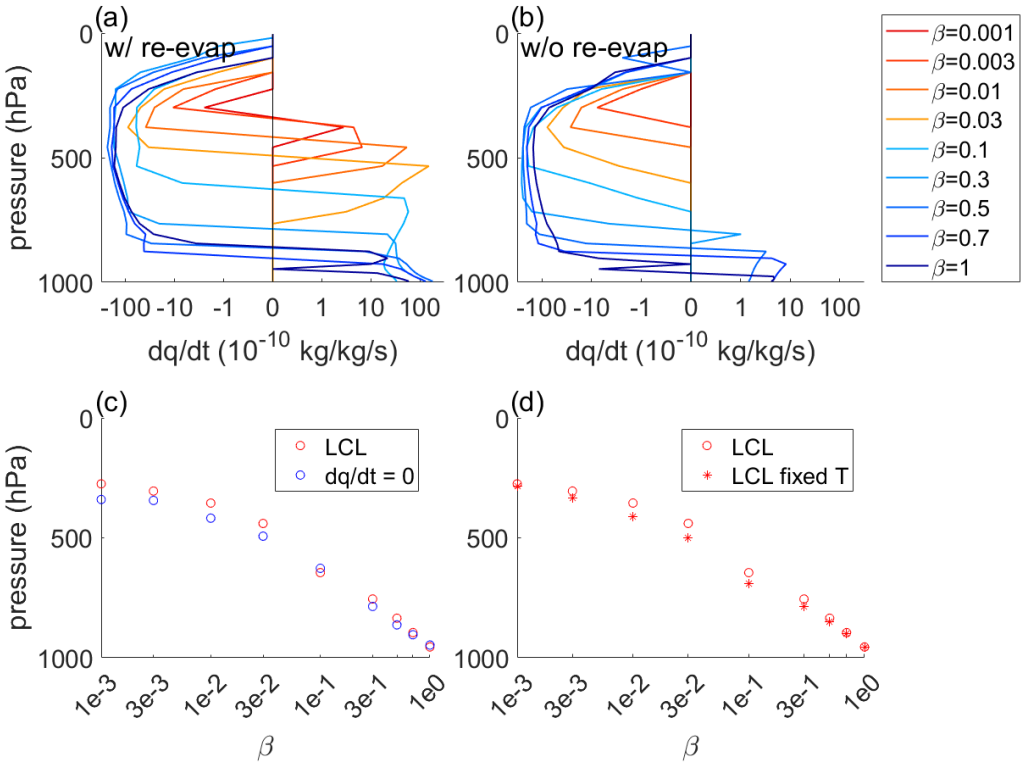

Figure 3. Moisture tendency from the stratiform precipitation scheme for simulations (a) with re-evaporation and (b) without re-evaporation. (c) Pressure where moistening tendency is zero with re-evaporation (blue circles) and lifting condensation level (red circles) predicted from Romps (2017) versus β. (d) Lifting condensation level versus β using surface relative humidity and temperature (red circles) and with surface temperature fixed at $\beta = 1$ (red stars).

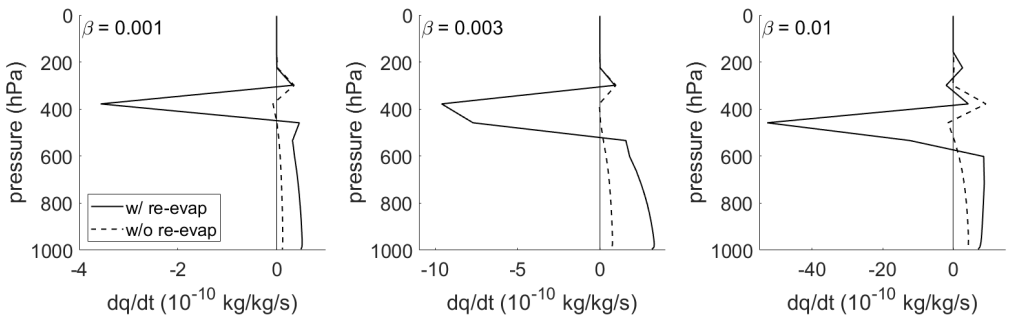

Figure 4. Moisture tendency from vertical diffusion for dry regime with re-evaporation (solid line) and without re-evaporation (dashed line). When re-evaporation is enabled, vertical diffusion transports moisture away (negative) from the lifting condensation level down to the near-surface (positive).

Table 1. The vertical length scale $\mathcal{H}$ estimated by assuming the moistening tendency from the stratiform precipitation scheme balances vertical diffusion [see equation (6)] is calculated from vertical diffusion (κ) and the time scale (τ). The time scale is calculated by dividing the specific humidity below the LCL (q) by maximum moisture tendency from re-evaporation of stratiform precipitation $(dq/dt)_{max}$. The actual vertical length scale $\mathcal{H}_{act}$ is calculated as the height where the moisture tendency from vertical diffusion is zero.

β	0.001	0.003	0.01
q (kg/kg)	4.37e-5	1.99e-4	1.09e-3
$(dq/dt)_{max}$ (10^{-10} kg/kg/s)	2.76	6.79	54.4
τ (hour)	44.0	81.6	55.8
κ (m^2/s)	1243	1132	892
$\mathcal{H}$ (km)	14.0	19.4	12.4
$\mathcal{H}_{act}$(km)	9.0	9.2	7.9

order as the actual scale, our scaling suggests diffusion can transport re-evaporated moisture to the near surface.

4 Summary and Discussion

We have studied the wet-to-dry regime transition of the tropical hydrological cycle in a general circulation model by reducing surface wetness. While the wet regime resembles the modern tropical climate, we find the dry regime corresponds to a scenario with negative tropical evaporation, which means the near-surface air has more moisture than the dry surface. By using a moisture budget analysis, the wet-to-dry regime transition is attributed to the difference between surface wetness and near-surface relative humidity. From mechanism denial experiments, we find re-evaporation of rain from stratiform clouds controls the regime transition: re-evaporation happens aloft near the LCL, which becomes higher as the surface dries out, then the moisture diffuses downward throughout the boundary layer. The role of vertical diffusion was confirmed using a scaling analysis that estimated the height assuming the moistening tendency is balanced by diffusion.

The importance of re-evaporation is unexpected but we do not believe it is an artifact of parameterized convection in our GCM. We find multiple similarities between our GCM results and the CRM results in Cronin and Chavas (2019). For example, in both cases reducing surface wetness leads to a deepening of the boundary layer and rising LCL, and the change of cloud fraction and precipitation flux are similar (compare Supplementary Fig. 5 to their Fig. 2). While we show re-evaporation from stratiform precipitation is the mechanism controlling the GCM regime transition, it is unclear whether a similar mechanism operates in the CRM, in which stratiform and convective precipitation are not explicitly distinguished. We expect further studies with resolved convection to re-examine the role of re-evaporation.

We demonstrate that our understanding of climate change between modern and warmer wet climates, which assume small changes in near surface relative humidity, does not hold for drier climates. In our simulations, the regime transition is determined by the difference between the surface and the atmosphere, so the relative humidity changes are important. Overall our aquaplanet simulations provide a first step to understanding the tropical hydrological cycle changes from wet to dry climates. Whether this regime transition is robust for other planetary climates remains unclear. More sophisticated lower

boundaries (e.g. land models, topography) are needed to extend the results beyond the modern climate regime.

Acknowledgments

B.F. and T. A. S. acknowledges support from National Science Foundation (AGS-1742944). The simulations in this paper were completed with resources provided by the University of Chicago Research Computing Center. Data necessary to reproduce the figures in this paper will be available via the University of Chicago's institutional repository Knowledge@UChicago (http://knowledge.uchicago.edu/record/2697?ln=en).

References

Abbot, D. S., et al. (2013). Robust elements of Snowball Earth atmospheric circulation and oases for life. *Journal of Geophysical Research: Atmospheres*, *118*(12), 6017-6027.

Anderson, J. L., et al. (2004). The new GFDL global atmosphere and land model AM2–LM2: Evaluation with prescribed SST simulations. *Journal of Climate*, *17*(24), 4641-4673.

Bacmeister, J. T., Suarez, M. J., & Robertson, F. R. (2006). Rain reevaporation, boundary layer–convection interactions, and Pacific rainfall patterns in an AGCM. *Journal of the Atmospheric Sciences*, *63*(12), 3383-3403.

Blackburn, M., & Hoskins, B. J. (2013). Context and aims of the aqua-planet experiment. *Journal of the Meteorological Society of Japan. Ser. II*, *91A*, 1-15.

Byrne, M., et al. (2018). Response of the Intertropical Convergence Zone to climate change: Location, width, and strength. *Current Climate Change Reports*, *4*, 355–370.

Cronin, T. W., & Chavas, D. R. (2019). Dry and semidry tropical cyclones. *Journal of Atmospheric Sciences*, *76*(8), 2193-2212.

Hartmann, D. L. (2016). *Global physical climatology (second edition).*

Held, I. M. (2018). 100 years of progress in understanding the general circulation of the atmosphere. *Meteorological Monographs*, *59*, 6.1-6.23.

Jakob, C., & Klein, S. A. (1999). The role of vertically varying cloud fraction in the parametrization of microphysical processes in the ECMWF model. *Quarterly Journal of the Royal Meteorological Society*, *125*(555), 941-965.

Kodama, T., Genda, H., O'ishi, R., Abe-Ouchi, A., & Abe, Y. (2019). Inner edge of habitable zones for Earth-sized planets with various surface water distributions. *Journal of Geophysical Research: Planets*, *124*(8), 2306-2324.

Kodama, T., Nitta, A., Genda, H., Takao, Y., O'ishi, R., Abe-Ouchi, A., & Abe, Y. (2018). Dependence of the onset of the runaway greenhouse effect on the latitudinal surface water distribution of Earth-like planets. *Journal of Geophysical Research: Planets*, *123*(2), 559-574.

Marshall, J. S., & Palmer, W. M. K. (1948). The distribution of raindrops with size. *Journal of Meteorology*, *5*, 165-166.

Moorthi, S., & Suarez, M. J. (1992). Relaxed Arakawa-Schubert. A parameterization of moist convection for general circulation models. *Monthly Weather Review*, *120*(6), 978-1002.

Pierrehumbert, R. T. (2002). The hydrologic cycle in deep-time climate problems. *Nature*, *419*, 191–198.

Pierrehumbert, R. T. (2005). Climate dynamics of a hard Snowball Earth. *Journal of Geophysical Research: Atmospheres*, *110*(D1).

Romps, D. M. (2017). Exact expression for the lifting condensation level. *Journal of Atmospheric Sciences*, *74*, 3891-3900.

Rotstayn, L. D. (1997). A physically based scheme for the treatment of stratiform clouds and precipitation in large-scale models. I: Description and evaluation

of the microphysical processes. *Quarterly Journal of the Royal Meteorological Society*, *123*(541), 1227-1282.

Schneider, T., Bischoff, T., & Haug, G. (2014). Migrations and dynamics of the intertropical convergence zone. *Nature*, *513*, 45–53.

Schneider, T., O'Gorman, P. A., & Levine, X. J. (2010). Water vapor and the dynamics of climate changes. *Reviews of Geophysics*, *48*(3), RG3001.

Tiedtke, M. (1993). Representation of clouds in large-scale models. *Monthly Weather Review*, *121*(11), 3040.

Toner, J. D., Catling, D. C., & Sletten, R. S. (2017). The geochemistry of Don Juan Pond: Evidence for a deep groundwater flow system in Wright Valley, Antarctica. *Earth and Planetary Science Letters*, *474*, 190-197.